

Supplementary Information

for

Tuning Electronic Structure for Enhanced Photocatalytic Efficiency:

Theoretical and Experimental Investigation of

$\text{CuM}_{1-x}\text{M}'_x\text{O}_2$ (M, M'=B, Al, Ga, In) Solid Solutions

Xian-Lan Chen^{1,3,#}, Bao-Feng Shan^{1,#}, Zong-Yan Zhao^{1,*}, Jin Zhang,² Qing-Ju Liu,^{2,*}

¹ Faculty of Materials Science and Engineering, Kunming University of Science and Technology,
Kunming 650093, P. R. China

² Yunnan Key Laboratory for Micro/Nano Materials & Technology, School of Materials and
Energy, Yunnan University, 650091 Kunming, P. R. China

³ School of Chemistry and Resources Engineering, Honghe University, Mengzi 661199, P. R.
China

The authors contribute equally.

* Corresponding author, E-mail: zzy@kust.edu.cn, qjliu@ynu.edu.cn

Thermodynamic stability

To schematize the thermodynamic solubility limit of $\text{CuM}_{1-x}\text{M}'_x\text{O}_2$, we compared their enthalpy of mixing (ΔH_{mix}) and the configurational entropy (ΔS_{mix}), ΔH_{mix} is defined as:

$$\Delta H_{\text{mix}}[\text{CuM}_{1-x}\text{M}'_x\text{O}_2] = E(\text{CuM}_{1-x}\text{M}'_x\text{O}_2) - xE(\text{CuM}'\text{O}_2) - (1-x)E(\text{CuMO}_2)$$

where $E(\text{CuM}_{1-x}\text{M}'_x\text{O}_2)$ is the total energy of $\text{CuM}_{1-x}\text{M}'_x\text{O}_2$ and $E(\text{CuM}'\text{O}_2)$ and $E(\text{CuMO}_2)$ are the total energies of ground states of $\text{CuM}'\text{O}_2$ and CuMO_2 .

ΔH_{mix} of $\text{CuAl}_{1-x}\text{Ga}_x\text{O}_2$ solid solutions can be reliably represented by a regular solution model, which has a symmetry of $x=0.5$. To capture the asymmetry of ΔH_{mix} with respect to composition of $\text{CuAl}_{1-x}\text{B}_x\text{O}_2$ ($0 \leq x \leq 0.417$), $\text{CuGa}_{1-x}\text{B}_x\text{O}_2$ ($0 \leq x \leq 0.167$), $\text{CuIn}_{1-x}\text{B}_x\text{O}_2$ ($0 \leq x \leq 0.167$), $\text{CuAl}_{1-x}\text{In}_x\text{O}_2$ and $\text{CuGa}_{1-x}\text{In}_x\text{O}_2$, a sub-regular solution model was used. The regular solution model and sub-regular solution model can be represented mathematically by the following equation:

$$\Delta H_{\text{mix}} = x(1-x)*\Omega(x)$$

$$\Delta H_{\text{mix}} = x(1-x)*[\Omega_1(1-x)+ \Omega_2x]$$

where x is the molar concentration, Ω is the interaction parameter.

$$\Omega(x,0.0 \text{ K}) = \Delta H_{\text{mix}}(x,0.0 \text{ K})/[x(1-x)]$$

The entropy of a solid solution is a sum of the configurational entropy (ΔS_{mix}) and the vibrations entropy. The vibrational entropy is negligible compared to ΔS_{mix} , ΔS_{mix} has a simple functional form.

$$\Delta S_{\text{mix}} = -k_B[x\ln x+(1-x)\ln(1-x)], k_B \text{ is a Boltzmann constant.}$$

The stability of solid solution is determined by the Gibbs-free energy of mixing (ΔG_{mix}), which includes not only ΔH_{mix} but also the contribution of ΔS_{mix} and temperature, which is given by:

$$\Delta G_{\text{mix}} = \Delta H_{\text{mix}} - T\Delta S_{\text{mix}} = (1-x)x* \Omega + k_B T[(1-x)\ln(1-x) + x\ln x]$$

where, ΔS_{mix} is positive and $-T\Delta S_{\text{mix}}$ is negative, indicating $-T\Delta S_{\text{mix}}$ has stabilizing effect. Moreover, from ΔG_{mix} , one obtains the solubility limits for binodal and spinodal decomposition, and the critical temperature as shown in **Figure 2b**.

The calculation of lattice mismatch

The lattice mismatch, $\Delta a/a$, and $\Delta c/c$ between CuMO_2 and $\text{CuM}'_x\text{O}_2$, can be calculated by the following equation:

$$\frac{\Delta a}{a} = \frac{|a_{\text{CuMO}_2} - a_{\text{CuM}'_x\text{O}_2}|}{a_{\text{CuMO}_2}}$$

$$\frac{\Delta c}{c} = \frac{|c_{\text{CuMO}_2} - c_{\text{CuM}'_x\text{O}_2}|}{c_{\text{CuMO}_2}}$$

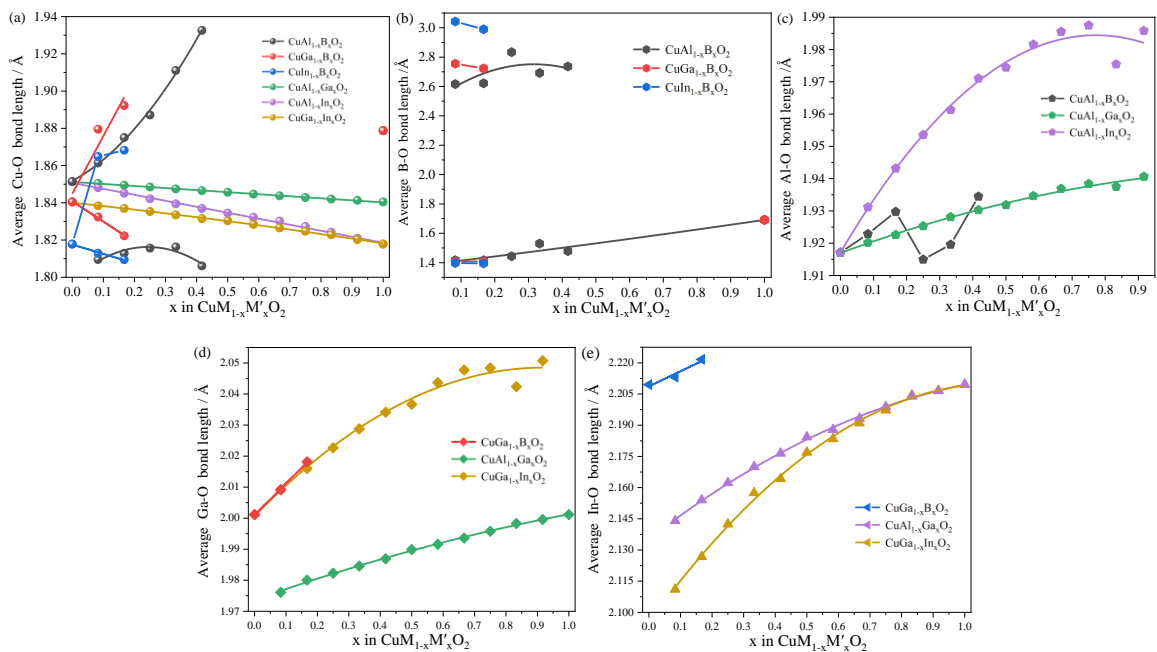


Figure S1. Average (a) Cu-O, (b) Al-O, (c) B-O, (d) Ga-O and (e) In-O bond lengths of $\text{CuM}_{1-x}\text{M}'_x\text{O}_2$ solid solutions as a function of content x .

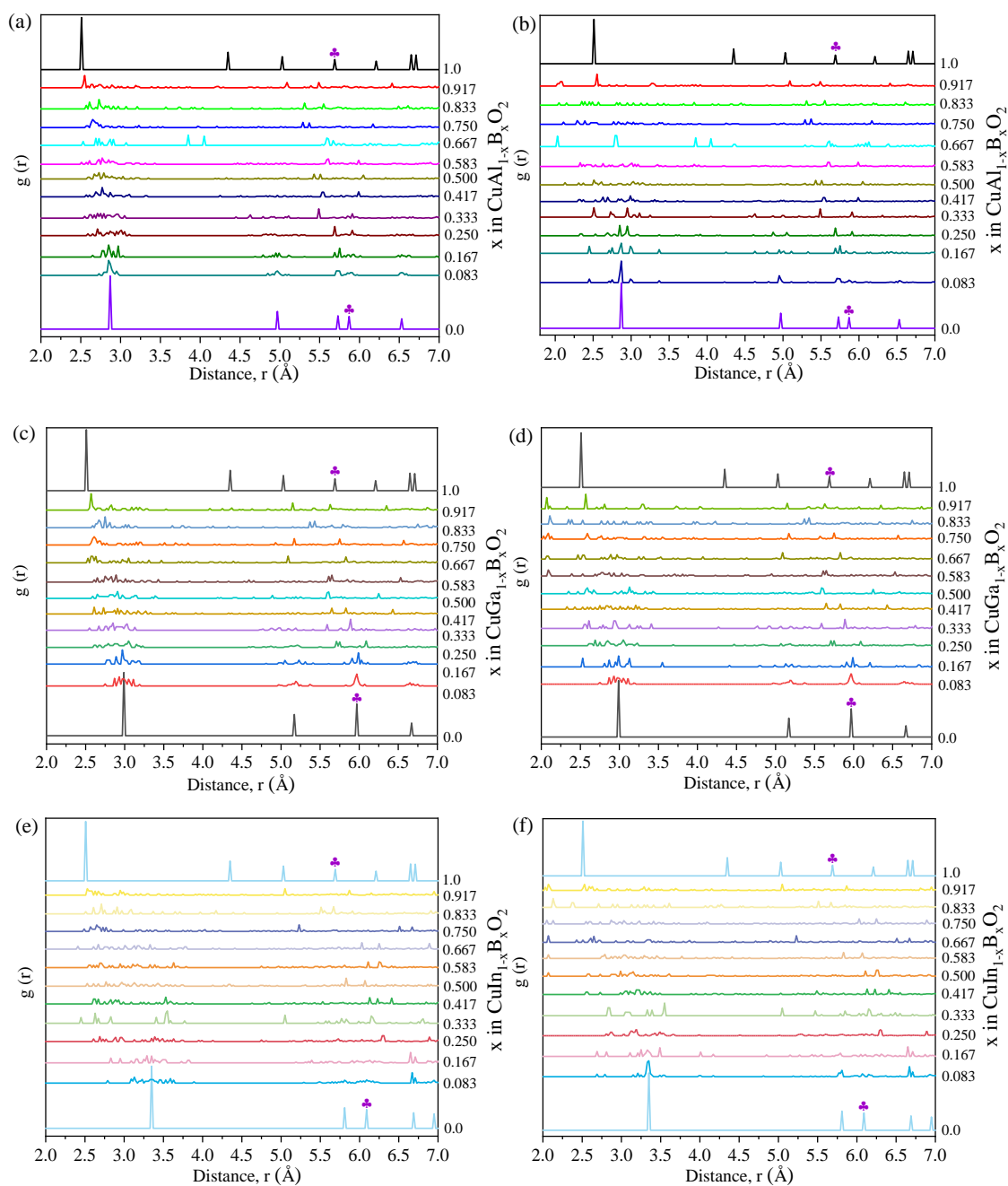


Figure S2. The partial radial distribution functions (a, c, e) Cu-Cu and (b, d, f) M-M average nearest neighbor occurrence vs distance for $\text{CuM}_{1-x}\text{B}_x\text{O}_2$ compounds, the corresponding RDF peaks of Cu-Cu and M-M in the nearest interlayer are marked with clubs.

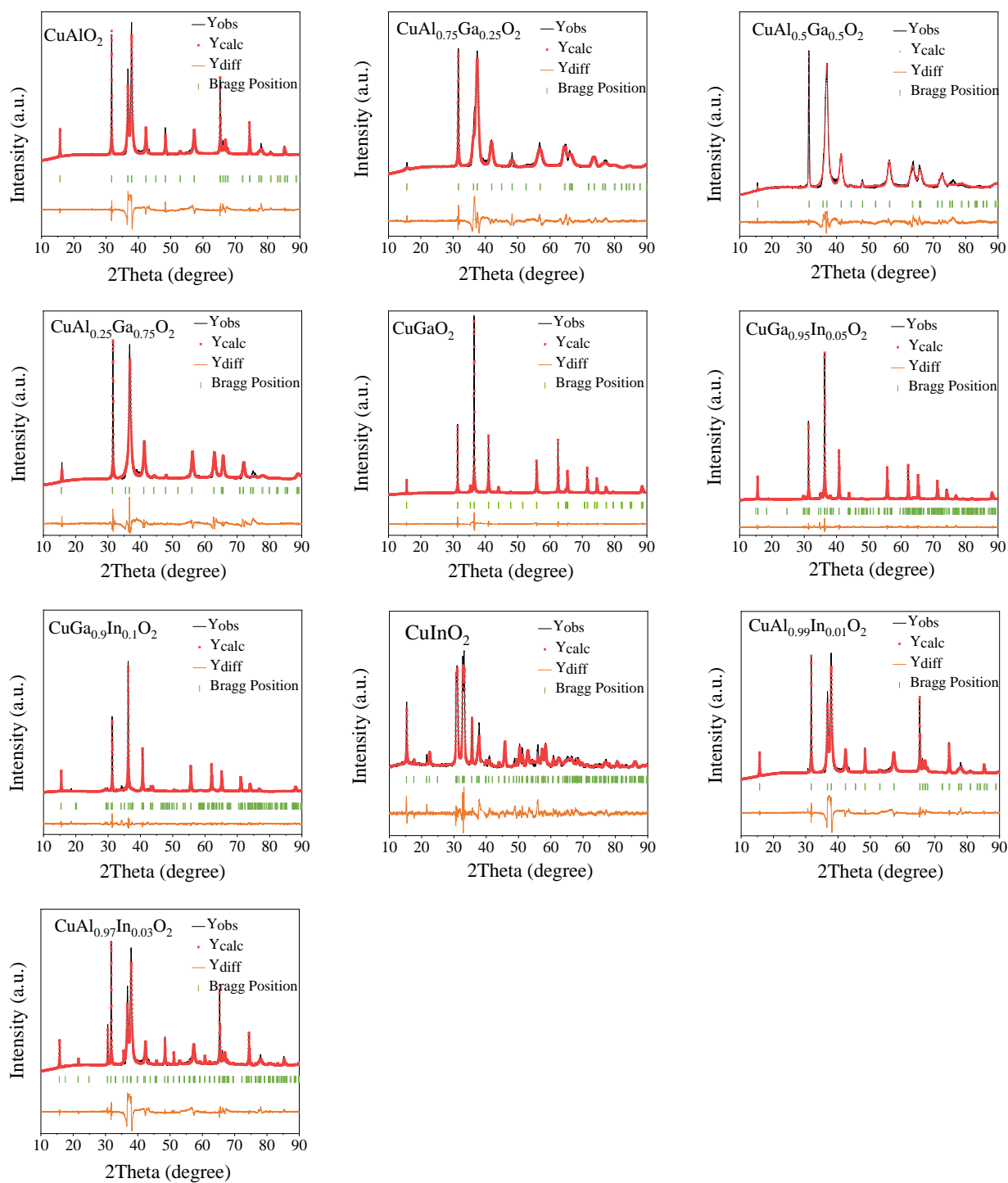


Figure S3. Powder X-ray diffraction and Rietveld plots of $\text{CuAl}_{1-x}\text{Ga}_x\text{O}_2$, $\text{CuGa}_{1-x}\text{In}_x\text{O}_2$ and $\text{CuAl}_{1-x}\text{In}_x\text{O}_2$ samples.

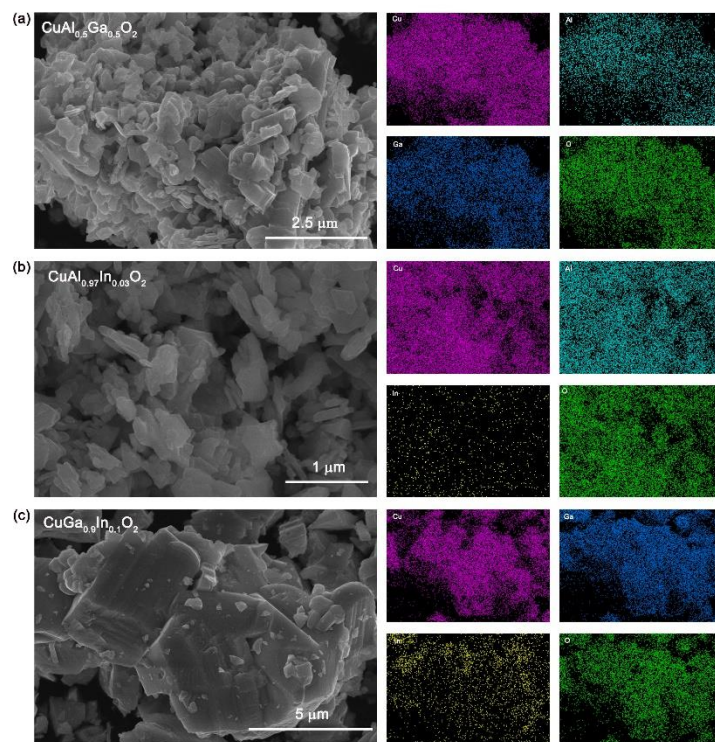


Figure S4. The SEM images and EDS element mappings of (a) $\text{CuAl}_{0.5}\text{Ga}_{0.5}\text{O}_2$, (b) $\text{CuAl}_{0.97}\text{In}_{0.03}\text{O}_2$, (c) $\text{CuGa}_{0.9}\text{In}_{0.1}\text{O}_2$ samples.

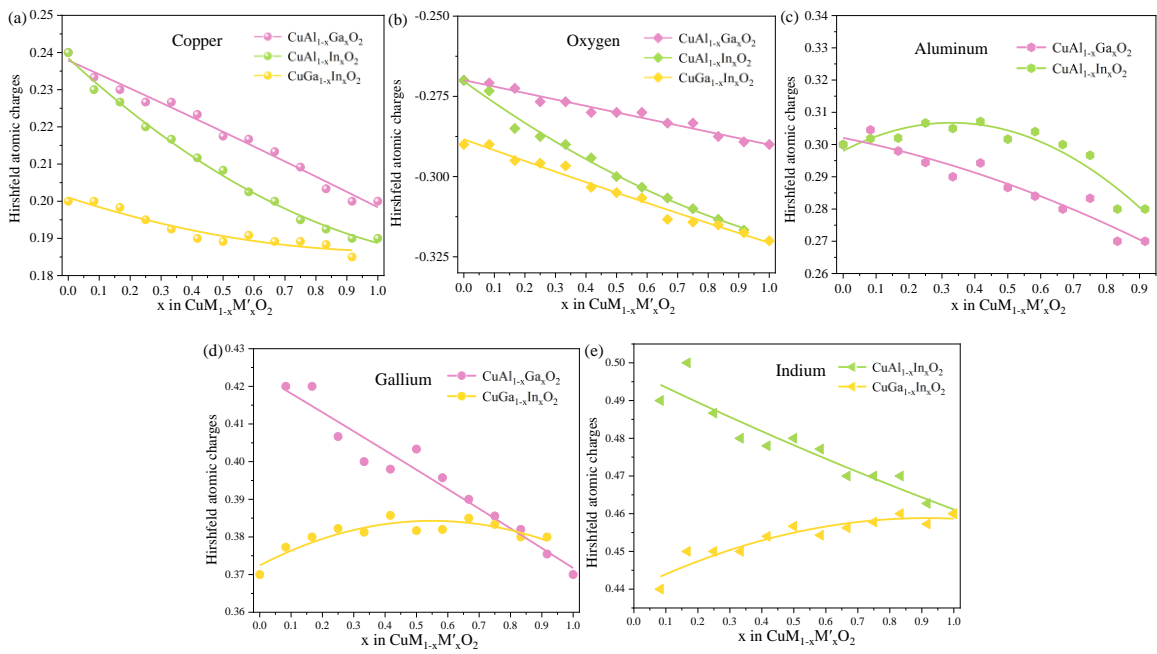


Figure S5. Average Hirshfeld charge Cu, O, Al, Ga and In atoms in $\text{CuM}_{1-x}\text{M}'_x\text{O}_2$ solid solutions.

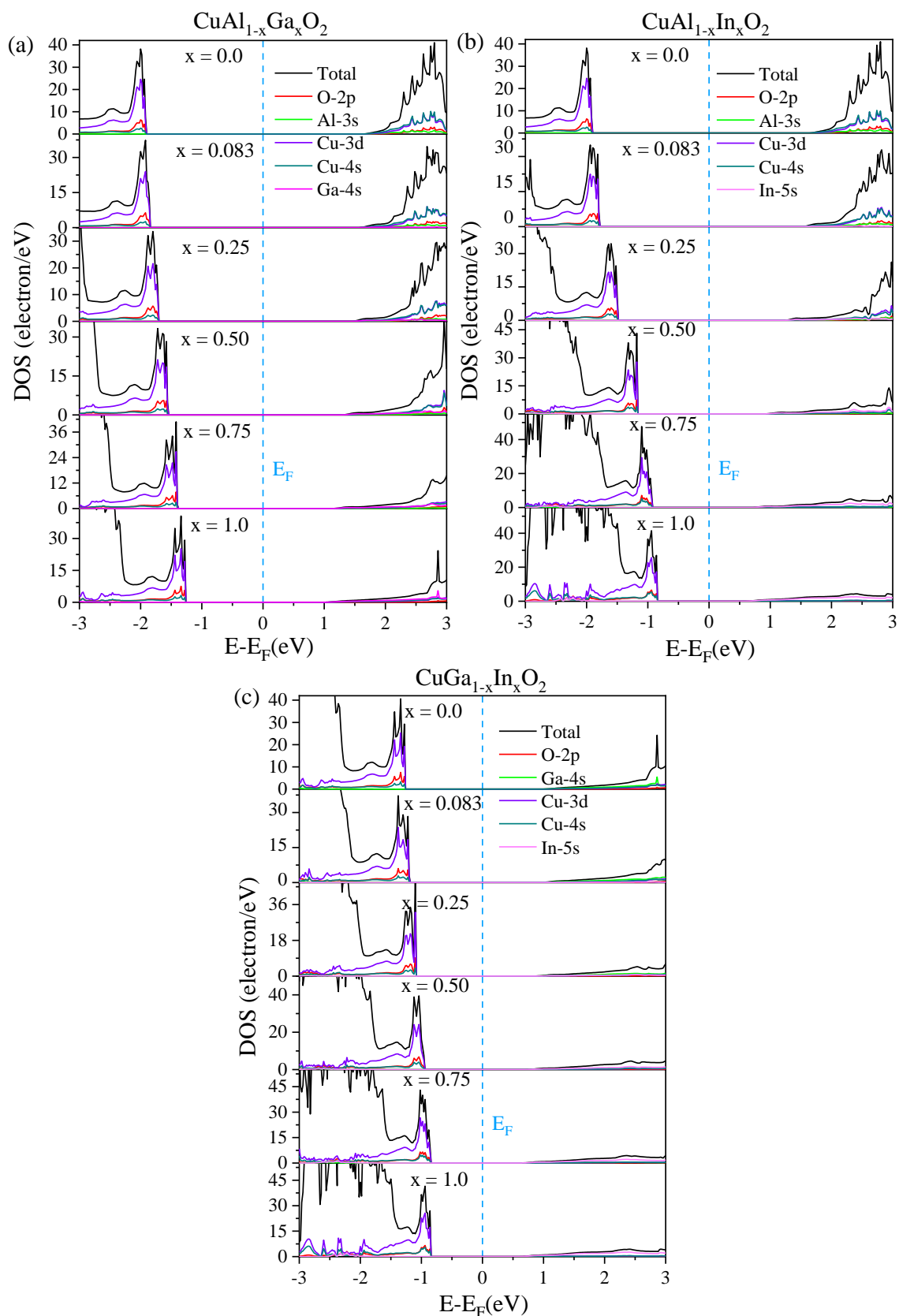


Figure S6. Projected density of states of $\text{CuAl}_{1-x}\text{Ga}_x\text{O}_2$, $\text{CuGa}_{1-x}\text{In}_x\text{O}_2$ and $\text{CuAl}_{1-x}\text{In}_x\text{O}_2$ solid solutions as a function of content x .

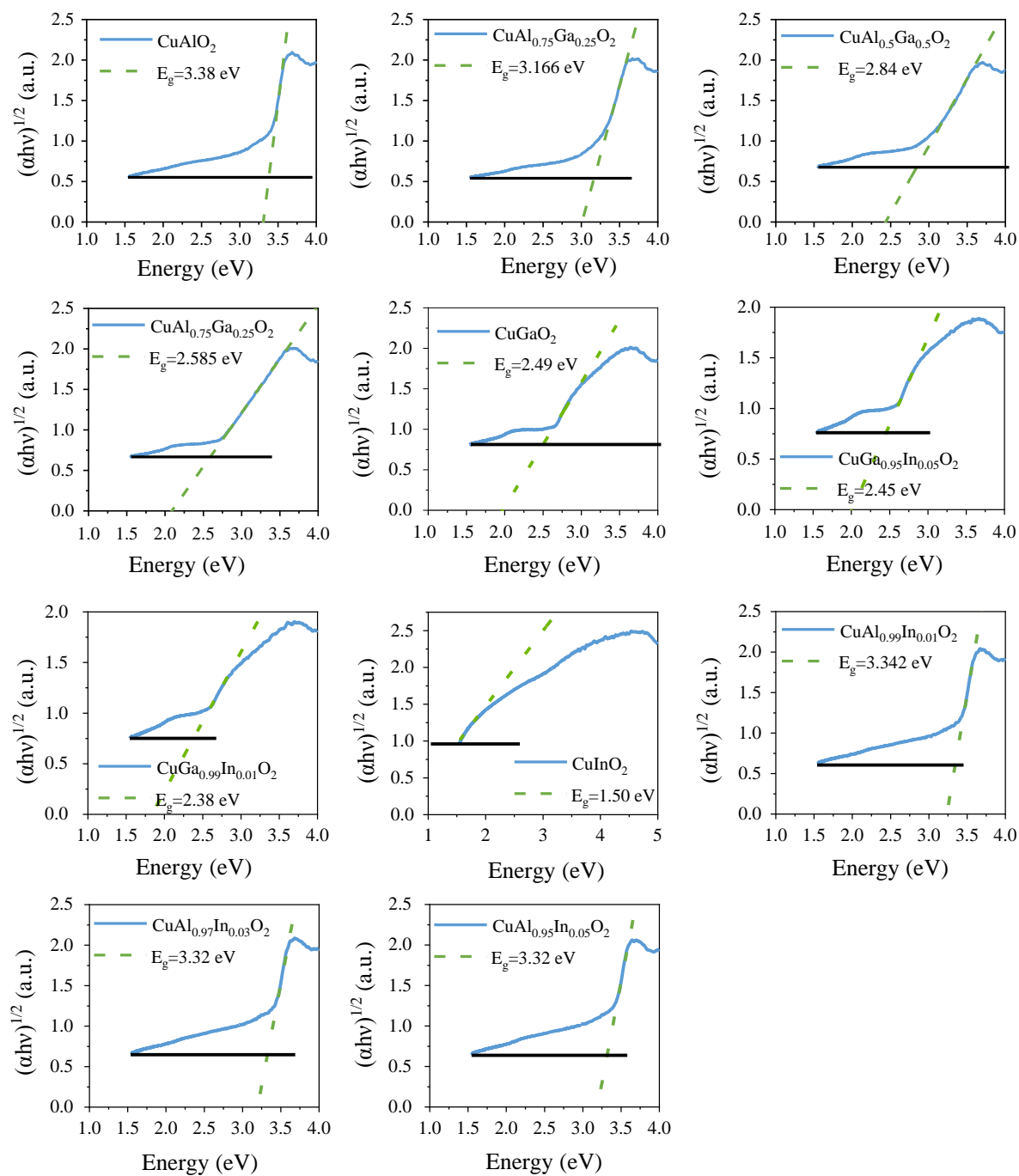


Figure S7. Optical band gaps of $\text{CuAl}_{1-x}\text{Ga}_x\text{O}_2$, $\text{CuGa}_{1-x}\text{In}_x\text{O}_2$ and $\text{CuAl}_{1-x}\text{In}_x\text{O}_2$ samples were estimated by the Tauc plot method.

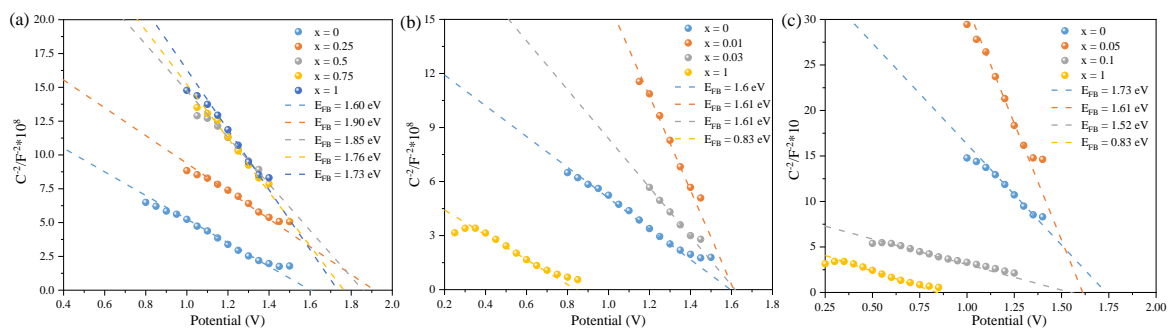


Figure S8. Mott–Schottky plots of $\text{CuAl}_{1-x}\text{Ga}_x\text{O}_2$ ($x=0, 0.25, 0.5, 0.75, 1$), $\text{CuAl}_{1-x}\text{In}_x\text{O}_2$ ($x=0, 0.01, 0.03, 1$) and $\text{CuGa}_{1-x}\text{In}_x\text{O}_2$ ($x=0, 0.05, 0.1, 1$) in aqueous Na_2SO_4 solution.

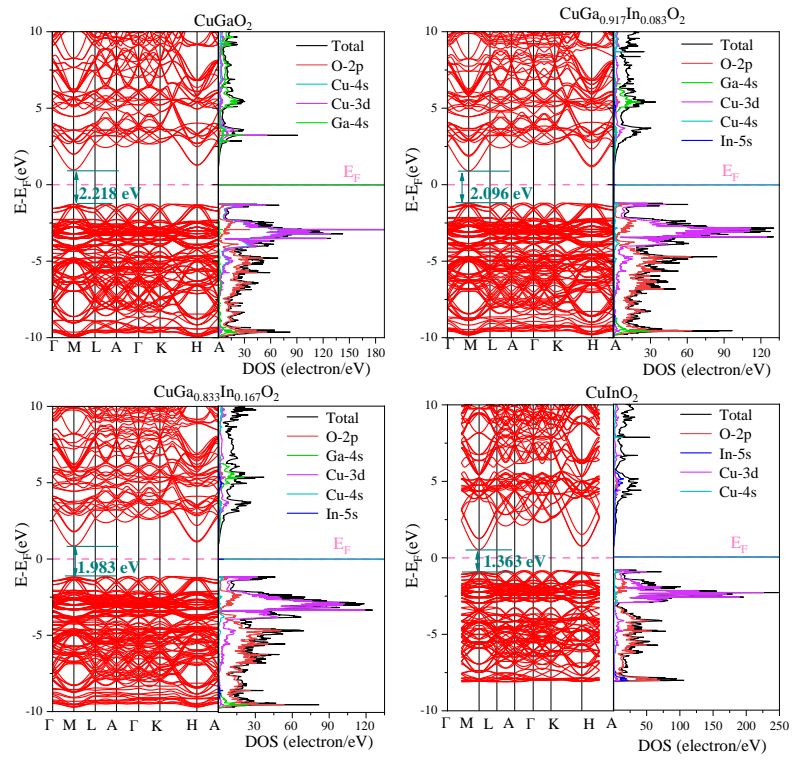


Figure S9. Band structure and the corresponding density of states of $\text{CuGa}_{1-x}\text{In}_x\text{O}_2$ solid solutions.

Table S1 The calculated lattice constants of CuBO₂, CuAlO₂, CuGaO₂ and CuInO₂.

	This work	Computational reference value		Experimental value/Å
	Lattice constants /Å	Lattice constants /Å	Computational method	
CuBO ₂	a=b=2.5117, c=16.5031	a=b=2.512, c=16.504 ²⁹ a=b=2.6, c=16.6 ³⁰	GGA- PBEsol PBE-GGA	a=b=2.53, c=16.58 (Pulsed laser deposition technique ³⁵)
	CuAlO ₂	a=b=2.8659, c=16.9179	a=b=2.861, c=16.978 ³¹ a=b=2.89, c=17.0 ³⁰	WIEN97 PBE-GGA
CuGaO ₂		a=b=2.9864, c=17.1373	a=b=2.9770, c=17.1710 ³² a=b=2.963, c=17.172 ³³	TB-LMTO LAPW
	CuInO ₂	a=b=3.3488, c=17.3237	a=b=3.34, c=17.5 ³⁰ a=b=3.359, c=17.529 ³⁴ a=b=3.2920, c=17.3880 ³³	PBE-GGA GGA-PBE TB-LMTO

Table S2. Rietveld refinement results of XRD pattern for all compositions of CuAl_{1-x}Ga_xO₂, CuGa_{1-x}In_xO₂ and CuAl_{1-x}In_xO₂ samples.

Material	Lattice parameter				
	a, b (Å)	c (Å)	α, β (°)	γ (°)	V (Å ³)
CuAlO ₂	2.8578	16.9288	90.0	120.0	119.8725
CuAl _{0.75} Ga _{0.25} O ₂	2.8883	16.9688	90.0	120.0	122.5952
CuAl _{0.5} Ga _{0.5} O ₂	2.9305	17.0566	90.0	120.0	126.8562
CuAl _{0.25} Ga _{0.75} O ₂	2.9616	17.1356	90.0	120.0	130.1631
CuGaO ₂	2.9766	17.1632	90.0	120.0	131.6990
CuAl _{0.99} In _{0.01} O ₂	2.8665	16.9384	90.0	120.0	119.6908
CuAl _{0.97} In _{0.03} O ₂	2.8783	16.9482	90.0	120.0	119.9165
CuInO ₂	3.3215	17.4000	90.0	120.0	166.2350
CuGa _{0.95} In _{0.05} O ₂	2.9894	17.1701	90.0	120.0	132.9590
CuGa _{0.9} In _{0.1} O ₂	2.9923	17.1724	90.0	120.0	133.1642
CuGa _{0.85} In _{0.15} O ₂	2.9919	17.1767	90.0	120.0	133.1579

Table S3. The atomic percentage of different cations extracted from SEM-EDS for $\text{CuAl}_{0.5}\text{Ga}_{0.5}\text{O}_2$, $\text{CuAl}_{0.97}\text{In}_{0.03}\text{O}_2$ and $\text{CuGa}_{0.9}\text{In}_{0.1}\text{O}_2$ samples.

Material	Atomic concentration from XPS				
	Cu (%)	Al (%)	Ga (%)	In (%)	O (%)
$\text{CuAl}_{0.5}\text{Ga}_{0.5}\text{O}_2$	26.1	13.2	13.8	0.0	47.3
$\text{CuAl}_{0.97}\text{In}_{0.03}\text{O}_2$	25.7	24.3	0.0	1.1	48.5
$\text{CuGa}_{0.9}\text{In}_{0.1}\text{O}_2$	21.7	0.0	25.8	2.4	50.1